Recent progress in air treatment with combined photocatalytic/plasma processes: A review

Lotfi Khezami, Phuong Nguyen-Tri, Wala Abdou Saoud, Abdelkrim Bouzaza, Atef El Jery, D Duc Nguyen, Vijai Kumar Gupta, Aymen Amine Assadi

Recent progress in air treatment with combined photocatalytic/plasma processes : A review

Lotfi Khezami[1,2], Phuong Nguyen-Tri[3]*, Wala Abdou Saoud[4], Abdelkrim Bouzaza[4], Atef El Jery [5] , D Duc Nguyen[6], Vijai Kumar Gupta[7], Aymen Amine Assadi[4*]

[1]LaNSER, Research and Technology Centre of Energy (CRTEn), BorjCedriaTechnopark, BP.95, Hammam-Lif 2050, Tunisia

[2]Department of Chemistry, College of Sciences, Imam Mohammad Ibn Saud Islamic University (IMSIU), P.O. Box 5701, Riyadh, 11432, Saudi Arabia

[3]Laboratory of Advanced Materials for Energy and Environment, Université du Québec à Trois-Rivières (UQTR), 3351, boul. des Forges, C.P. 500, Trois-Rivières (Québec) G9A 5H7 Canada

[4]Univ Rennes, École Nationale Supérieure de Chimie de Rennes (ENSCR), Centre National de la Recherche Scientifique (CNRS), UMR 6226, 11 allée de Beaulieu, 35708 Rennes, France

[5]Department of Chemical Engineering, College of Engineering, King Khalid University, Abha 61411, Saudi Arabia

[6]Department of Environmental Energy Engineering, Kyonggi University, Room 410, 2nd Engineering Building,154-42, Gwanggyosan-ro, Yeongtong-gu, Suwon-si, Gyeonggi-do 16227, Korea

[7]Biorefining and Advanced Materials Research Center, Scotland's Rural College (SRUC), Kings Buildings, West Mains Road, Edinburgh EH9 3JG, UK

* Corresponding authors:

Email : Aymen.assadi@ensc-rennes.fr (A. A. Assadi); Tel.: +33 2 23238152

Email: Phuong.Nguyen-Tri@uqtr.ca (P. Nguyen-Tri); Tel : + 819 376-5011 (4505)

Abstract

Nowadays, air pollution is an increasingly important topic, as environmental regulations require limiting pollutant emissions. This problem requires new techniques to reduce emissions by either improving the current emission control systems and processes or installing new hybrid treatment systems. These are of broad diversity, and every system has its advantages and disadvantages. The tendency is, accordingly, to combine various techniques to achieve more acceptable and suitable treatment. Recent studies suggest that the combination of photocatalysis and plasma in a reactor can offer attractive pollutant treatment efficiency with a minimum of partially oxidized by-products than that of these processes taken separately. However, there is little review of the capability of this pairing to treat different brands of pollutants. Besides, available data concerning reactor design with flows treated 10 to 1000 times higher than those studied at the lab scale. This review paid particular attention to determine the reaction mechanisms in terms of engineering and design of combination reactors (plasma and catalysis). Likewise, we developed the effect of critical parameters such as pollutant load, relative humidity, and flow rate to understand the degradation kinetics of specific pollutants individually by using plasma and photocatalysis. Additionally, this review compares different designs of cold plasma reactors combination with heterogeneous catalysis with special attention on synergistic and antagonistic effects of using plasma and photocatalysis processes at the laboratory, pilot, and industrial scales. Therefore, the elements discussed in this review stick well to the first theme on pollution prevention of the special issue concerning pollution prevention and the application of clean technologies to promote a circular (bio) economy.

Keywords: Process extrapolation, Air pollution; Non-thermal plasma; photocatalysis; Synergetic effect

1. Introduction

The increasing emission of volatile organic compounds (VOCs) into the atmosphere is a major public health concern today (Zhang, 2018; Tong, 2019; Li et al., 2018). Many studies have shown that exposure to VOCs can be toxic, carcinogenic, mutagenic, or teratogenic (Zhang, 2018; Sun et al., 2021; Tong, 2019; Li et al., 2018). Air pollution causes respiratory illnesses, allergies, cardiopulmonary diseases (e.g., asthma and myocardial infarction), reduced fertility, increased infant mortality, weakened immune system, and several other health hazards in humans. However, the adverse impacts of air pollution on public health depend on the magnitude of pollution, contaminant type, age group of exposed individuals, geographical region, and climatic/weather conditions, to name a few. It should be noted that the elderly individuals, children below 12 years and immunocompromised persons, and people with underlying medical conditions are more acute to illnesses caused by air pollution (Annesi-maesano et al., 2011).

In addition to their direct effects on health, many compounds have low odour thresholds in the polluted air and cause a significant nuisance to the exposed personnel and neighbourhood. Eliminating odour nuisance is a complex subject because the principle often lies in treating a low-load high-flow effluent, but is made up of many chemical compounds, each of which contributes to the odorous color. The prominent families are sulfur derivatives (e.g., hydrogen sulfide, mercaptans, and sulfides), nitrogen (e.g., ammonia and amines), and oxygen (e.g., volatile fatty acids, alcohols, aldehydes, and esters).

Different techniques for eliminating pollution in gaseous discharges are divided into two main classes : (i) pollutant adsorption or absorption and (ii) pollutant degradation. Adsorption and/or absorption chiefly capture the contaminant from the atmosphere or a specific gas phase by re-encrypting them in another fluid phase (via absorption) or solid support (via adsorption). Pollutants are captured and concerted in one location. Nonetheless, this necessitates an operation of regeneration of the transfer medium for the second cycle. The latter can be realized, for example, by coupling the transfer of pollutants by absorption with a biological treatment unit. On the other hand, the destructor techniques or the oxidation processes, based on chemical reactions to eliminate pollution, are marked by forming sub-intermediate products of H_2O and CO_2. This reaction is carried out under controlled conditions such as those involving high temperatures (e.g., combustion) or mild to moderate temperatures (e.g., cold plasma and catalytic oxidation).

This review focuses on (i) comparing different designs of cold plasma combined reactors with heterogeneous catalysis (ii) to the synergistic and antagonistic effects of using plasma and photocatalysis processes at the laboratory, pilot, and industrial-scale (iii) reasons of this synergtic effect. To our knowledge, no review papers approach these aspects with a comprehensive vision at different scales. Furthermore, particular attention has been paid to determining the reaction mechanisms in engineering and combined reactors design (plasma and catalysis). Moreover, we have developed the effect of critical parameters such as pollutant load, relative humidity, and flow rate to understand the degradation kinetics of specific pollutants individually using plasma and photocatalysis.

2. Non-thermal plasma technology

A state of matter, plasma, consists of ionizable gases obtained by heat, excitation, or electromagnetic conditions. The plasma is generated through the combination of neutral species, positive ions, and electrons. Plasma in air produces filamentary plasmas, which are excellent sources of radicals and excited species that form a globally oxidizing medium, even at low injected energy. The reactivity of these plasmas is demonstrated here too on a considerable number of organic molecules, i.e, thermal plasma exhibits extremely high equilibrium temperatures. Moreover, the temperature of the electrons can be greater than that of the gas phase, which has an almost ambient temperature (e.g., cold plasma). At high ionization energy, the electrons react directly with the molecules and ions existing, ensuring the formation of excited compounds and radicals that, in turn, allow them to oxidize the pollutants present in the air at room temperature (Tong, 2019). Various categories of discharge are used to generate cold plasmas. Plasma with dielectric barrier discharge (DBD) and corona discharge are commonly applied to mitigate air pollution (Zhang, 2018; Tong, 2019).

(i) **Plasma with Corona discharge**: This discharge occurs by applying a difference in high potential (some tens of kV) of two electrodes with variable curvatures. Wire-plane, point-plane, and fill-cylinder type geometries are mainly used for plasma with corona discharge. The curved electrode initiates the electric discharge, which further progresses in the proximity of the planar counter electrode.

(ii) **Plasma with dielectric barrier discharge (DBD)**: To generate DBD, dielectric barriers such as specific isolating material or supports (Annesi-maesano et al., 2011; D.P. Subedi, U.M. Joshi, 2017), e.g., ceramic, quartz, glass, or Teflon are used to separate the two electrodes. Various

configurations are available for DBD, such as coaxial cylinders, plane-plane, plane-wire, and plane-point type. Depending on the type of dielectric barrier and the electrodes' offset arrangement, DBD can be classified into volume DBD plasma or a surface DBD plasma depending on the type of dielectric barrier and the electrodes offset arrangement. In Fig. 1, a non-exhaustive list of some different configurations of cylindrical and planar plasma DBD reactors is provided.

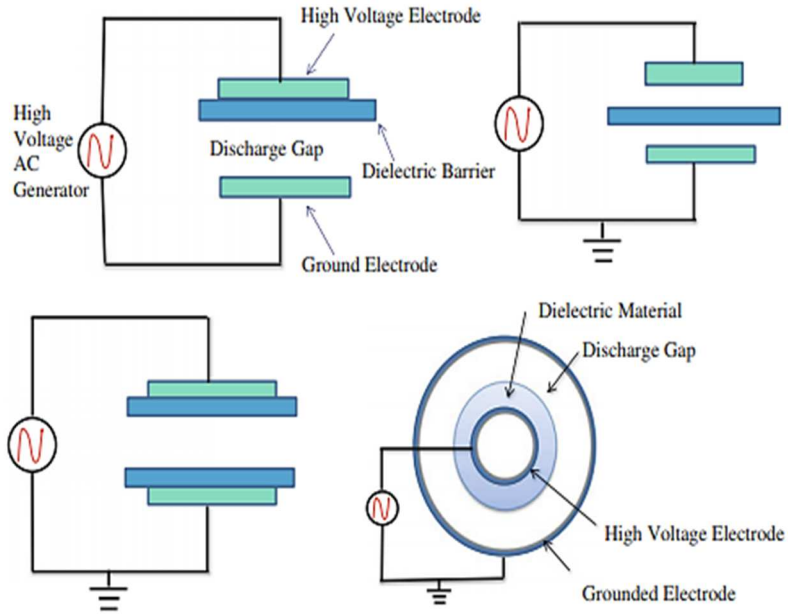

Figure 1. Some configurations of DBD plasma (Zhang, 2018)

Ideal and conducive to prevent the generation of undesired and toxic by-products, the pollutants must be oxidized with total mineralization marked by the formation of CO_2 and H_2O. However, on a practical level, plasma reactors allow partial degradation with a significant formation of oxidized by-products, which are sometimes not identified in the treated emanation, likely generating additional problems than the initial pollutant (Zhang, 2018; Durme et al., 2008). Moreover, non-thermal plasma alone has drawbacks regarding energy efficiency and by-product generation presented with poor CO_2 selectivity even at high conversion rates (Zhang,

2018). The presence of ozone and nitrogen oxides in the effluents leaving non-thermal plasma air treatment systems constitutes this technology's biggest drawback, which will require post-treatment to eliminate these toxic by-products and more, particularly, ozone. The association of another remediation method and the plasma makes it possible to combine their destruction efficiency and to limit the drawbacks of each process (Jiang et al., 2017; Schiavon et al., 2017).

Recently, many investigators have focused on evolving the mineralization to have complete oxidation while combining cold plasma with catalysts (Jiang et al., 2017; Schiavon et al., 2017). Numerous catalysts have been experienced, in the literature, using diverse categories with different pollutants (e.g., ammonia, hydrogen sulfide, and VOCs). Undeniably, the coupling of the cold plasma and the photo-catalyst has shown better performance than the efficiency of each process when taken separately. Consequently, this review explores the synergistic effects of using the combination of photocatalysis and cold plasma techniques for pollutant degradation.

3. Photocatalytic reactors

A semiconductor can absorb light radiation to promote an electron from the valence state to the conduction band while creating a hole (h+) in the valence band as a photo-catalyst. Most of the resulting electron-hole (e-/h+) pairs recombine, whereas a few others can oxidize or reduce the compounds adsorbed on the catalytic surface (Neyts, 2016). These reactions can occur directly in the presence of the specific pollutant or indirectly with the aid of oxygen and water in the atmosphere to yield their radicals such as $O_2^{\circ-}$ and HO° (Saoud et al., 2020 & 2021; Almomani et al. 2020). These reactive oxygen species (ROS) are highly selective for oxidation and

168 mineralization of the pollutants (Assadi, 2012; Boyjoo et al., 2017). The most
169 commonly investigated photo-catalyst is TiO_2 that absorbs the wavelength of
170 ultraviolet (UV) radiation of less than 388 nm (Elfalleh et al., 2017). Table 1
171 summarizes some notable studies on eliminating various volatile organic compounds
172 (VOCs) in a photocatalytic reactor, such as aromatics, aldehydes, and mercaptans.

173 **Table 1. Reactor configuration for pollutant removal**

Target pollutants	Reactor design	References
Acetylene	Continuous reactor	(Thevenet et al., 2014)
Tetrachloroethylene and Decane	Annular reactor	(Monteiro et al., 2015)
Ethanol et Benzene	Batch reactor	(Andryushina and Stroyuk, 2014)
Isopropanol	Tubular reactor	(Hou and Ku, 2013)
Cyclohexane	Fixed bed reactor	(Murcia et al., 2013)
Benzene	Fixed bed reactor	(Zhuang et al., 2014)
Toluene	Continuous and batch reactors	(Pham and Lee, 2015, Almomani et al., 2020)
Acetone and benzene	Batch reactor	(Xie et al., 2015)
Dichloromethane	Batch system combined with (bio)reactors	(Almomani et al., 2021)
Trimethylamine	Annular reactor	(Assadi et al., 2012)
Isovaleraldehyde	Planar and cylindrical reactor	(Assadi et al., 2014c; Palau et al., 2015)
Formaldehyde	Fixed bed reactor	(Han et al., 2013)
Butyraldehyde	Planar reactor	(Ghaida et al., 2016)
Dimethyl disulfide	Planar reactor Cylindrical reactor	(Chuang and Luo, 2013; Saoud et al., 2017)
Dimethyl sulfide	Annular reactor	(Lin et al., 2016)
2, 3 Butadione	Planar reacor with luminous	Saoud et al., 2021

	textiles	
NOx	Tubular reactor, Fixed bed reactor Rectangular reactor	Hu et al., 2015; Ma et al., 2015; Szatmáry et al., 2014)
H_2S	Tubular reactor	(Alonso-tellez et al., 2014)
	Planar reactor	(Portela et al., 2010)
SO_2	Fixed bed reactor	(Liu et al., 2014)
NH_3 & H_2S	Rectangular reactor	(Maxime and Amine, 2014)

Some inorganic pollutants such as ammonia, NO_X, SO_X, CO, and H_2S, mainly from the industrial sector, are also eliminated by the photocatalysis reactor. Nevertheless, compared to previous studies (Table 1), these ranges of molecules are less studied.

An advantage of heterogeneous photocatalysis is its ability to mineralize a wide range of organic compounds in water and air. Several researchers have widely studied its efficiency in degrading different molecules (Assadi, 2012; Boyjoo et al., 2017; Saoud et al., 2020). The most commonly studied families of organic compounds are chlorinated compounds (Monteiro et al., 2015), phenols (Bechec et al., 2015; Murcia et al., 2013; Pham and Lee, 2015; Xie et al., 2015; Zhuang et al., 2014), nitrogen compounds (Assadi et al., 2012) and sulfur compounds (Chuang and Luo, 2013; Lin et al., 2016; Saoud et al., 2017). The photocatalytic reaction can be activated by photon irradiation and operate at room temperature and atmospheric pressure with reasonable installation requirements (Andryushina and Stroyuk, 2014; Assadi et al., 2012, 2014c; Bechec et al., 2015; Chuang and Luo, 2013; Ghaida et al., 2016; Han et al., 2013; Hou and Ku, 2013; Lin et al., 2016; Monteiro et al., 2015; Murcia et al., 2013; Palau et al., 2015; Pham and Lee, 2015; Saoud et al., 2017; Thevenet et al., 2014; Xie et al., 2015; Zhuang et al., 2014). However, the

advantages of photocatalysis are hampered by some significant drawbacks. The photo-catalyst is only activated by UV irradiation, limiting its effectiveness in the visible and interior applications (Palau et al., 2015). The recombination of photogenerated charges between their formation and diffusion on the semiconductor surface can also decrease the process efficiency.

Abou Saoud et al. confirmed the poisoning of photocatalysis for sulfur and nitrogen pollutants at the pilot-scale (Saoud et al., 2017). The authors showed that, after many photocatalysis self-regeneration procedures, the photocatalytic efficiency reduced considerably (Saoud et al., 2017). Therefore, a poisoning phenomenon may be evident during a continuous and prolonged photocatalytic oxidation process. To remedy these problems and increase photocatalytic activity, a combination of photo-catalyst and other processes such as non-thermal plasma could be helpful (Ramaraju and Subrahmanyam, 2014; Dou et al. 2016; Mei et al. 2016; Assadi et al. 2016; Aouadi et al.2016; Maciuca et al. 2012; Karuppiah et al. 2013; Huang et al., 2010; Jo et al., 2016; Karuppiah et al. 2014; Assadi et al. 2015; Pham Huu et al. 2017).

4. Plasma/photocatalytic hybrid systems

Based on each process considered alone (plasma or photocatalysis), TiO_2 is a catalyst capable of oxidizing many organic molecules with excellent selectivity to CO_2, thanks to its quantum efficiency and the redox potentials of its valence and conduction bands. In recent years, many studies combining the non-thermal plasma (e.g., dielectric barrier discharge - DBD, corona discharge, and surface discharge) and catalysts are carried out on different types of effluents, thus highlighting the existence of a synergistic effect due to the coupling process (Karuppiah et al. 2014; Assadi et al. 2015; Pham Huu et al. 2017). TiO_2 is a catalyst capable of oxidizing

many organic molecules into CO_2 with excellent selectivity. Plasma DBD in air produces ionized filaments that are excellent sources of radicals and excited species that form a globally oxidizing environment even at room temperature and low input energy (Saoud et al., 2017). Non-thermal plasma presents remarkable performances (e.g., conversion efficiency and energy cost) for low polluted effluents (Saoud et al., 2017; Dou et al. 2016; Mei et al. 2016). The major challenge with the plasma is to avoid the formation of oxidation by-products and to pursue the reactions towards total mineralization (Zhang, 2018; Trinh and Mok 2015a; Liu et al., 2014; Maxime and Amine, 2014). TiO_2, due to its adsorption capacity, tends to maintain the by-products in an adsorbed state, thus exposing them to the long-lived radicals to achieve their full degradation (Trinh and Mok 2015a). It is interesting to correct these types of plasma defects by supplying TiO_2 (Schiavon et al., 2017).

Considering the ability of photocatalysis to reach a high mineralization rate, various investigations have been performed combining the later and non-thermal plasma, to heighten the elimination with consistently complete mineralization. A few studies in this area have recently shown the application of a broad set of reactor configurations permitting the association of the plasma and photocatalytic processes for pollutant denaturation. The different reactor configurations reported in the literature are summarized in this section. Some recent studies (Saoud et al. 2019; Patil et al. 2016; Jo et al. 2016; Nguyen Dinh et al. 2015; Li et al., 2015; Ramaraju and Subrahmanyam, 2014; Saoud et al., 2017; Trinh and Mok, 2015a) on the catalyst performance and its association with the plasma discharge have remarkable impacts on the rate of VOCs elimination and the mineralization effectiveness (Zadi et al., 2018). Nevertheless, the in-situ characterization of these hybrid processes with an active plasma is rarely investigated due to the convoluted experimental reactor

241 configurations to associate the plasma, performance monitoring tools and analytical
242 facilities (Figure 2)

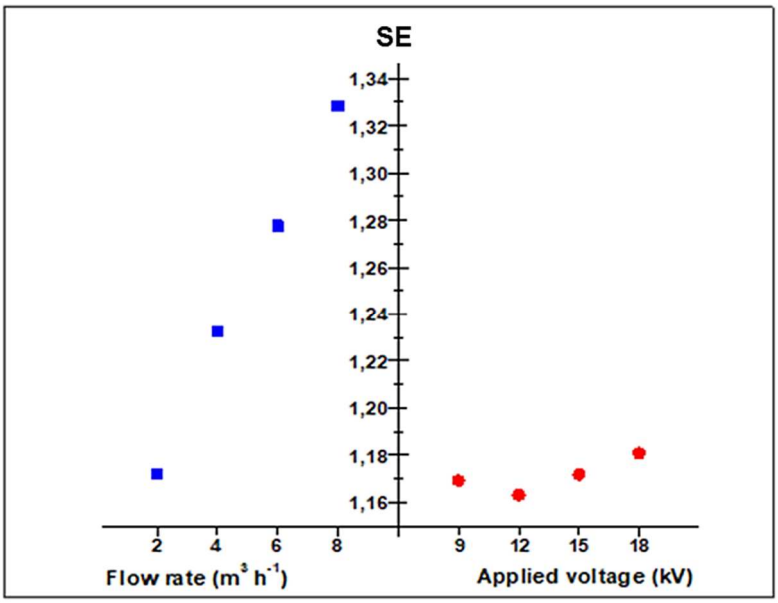

243

244 **Figure 2:** Example of Variation of synergetic effect (SE) with flow rate (at V= 15 kV)
245 and applied voltage (at Q= 2 m^3 h^{-1}) using three processes (Zadi et al., 2018)

246 **4.1 Design of hybrid plasma/photocatalytic systems**

247 Several investigations show that the interesting reactors configurations about
248 plasma combined with photocatalysis were about DBD (Schiavon et al. 2017; Huang
249 et al., 2010; Jo et al., 2016; Ramaraju and Subrahmanyam, 2014; Zhu et al., 2015a;
250 Shi et al., 2016; Jiang et al., 2017a; Chen et al., 2016; Jo et al., 2016; Bahria et al.,
251 2016) and corona discharge (Shirjana et al 2020; Nan et al 2016; Changming et al
252 2019; Wan et al. 2011; Mikhail et al. 2016; Fada et al. 2015; Sultana et al. 2019 ;
253 Vandenbroucke et al. 2016; Nguyen Dinh et al. 2015). Moreover, some authors have
254 extensively documented that DBD release is relatively more effective compared to
255 corona release because of the uniformity in plasma discharge on the catalyst surface
256 (Ramaraju et al., 2013). Several configurations are promising to provide a solution to

this problem. The coupling between plasma by dielectric barrier discharge (DBD) and TiO_2/UV photocatalysis reveals exciting configurations in terms of synergy to destroy VOCs with low energy consumption (Aouadi et al., 2016). Recent work on model compounds indicates that this association needs to be explored and developed. Associating a photo-catalyst in a DBD that produces filamentary plasmas in the air, which are excellent sources of radicals and excited species, will make it possible to intensify the oxidizing environment with the same injected energies. The reactivity of these systems has been demonstrated on a large number of organic molecules (Fig. 3) (Assadi et al. 2018; Chen et al. 2016; Karuppiah et al. 2014).

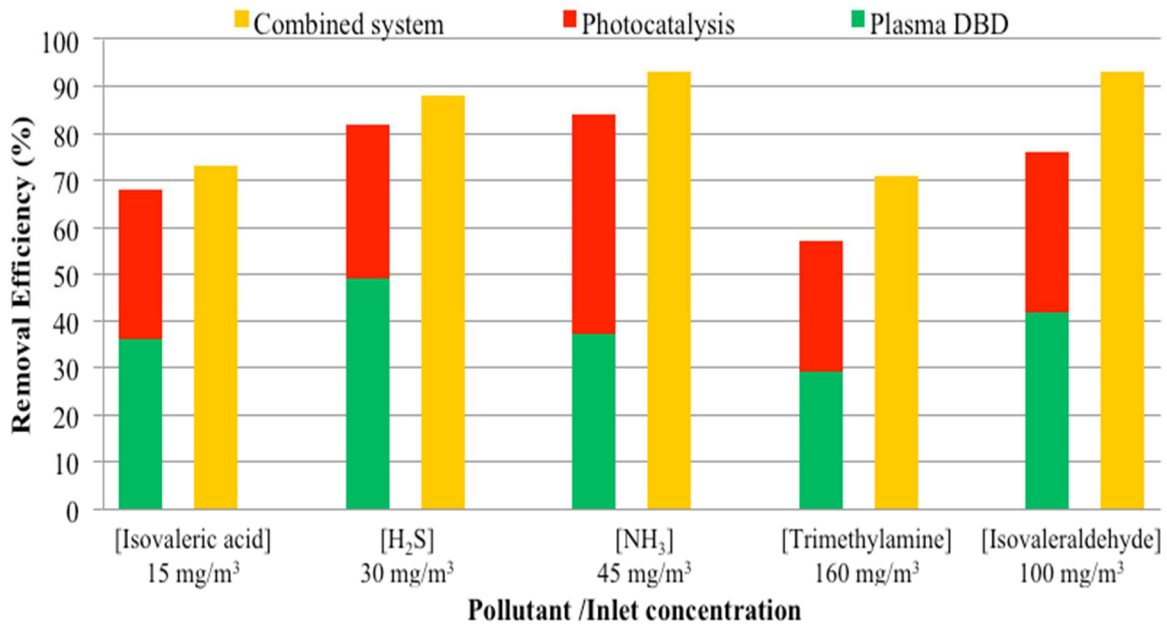

Figure 3: Example of the synergistic effects of plasma-photocatalysis for the degradation of isovaleric acid, hydrogen sulfide, ammonia, trimethylamine and isovaleraldehyde (Assadi, 2012)

4.2 Catalyst type and its function in plasma discharge

The catalysts have been positioned in two important ways to elucidate the functionality of different active species generated by plasma upon catalyst activation.

Firstly, the catalyst is introduced into the discharge zone (in-plasma catalysis, IPC) (Patil et al. 2016; Jo et al. 2016; Xu et al. 2016; Chen et al. 2016; Pham Huu et al. 2017; Zhu et al. 2015a). Secondly, the gas phase moves to the discharge zone before encountering the catalyst, which is then installed downstream (post-plasma catalysis, PPC) (Assadi et al. 2018; Huang et al., 2010; Nguyen Dinh et al. 2015; Li et al. 2015; Vandenbroucke et al. 2016). According to some reports, the IPC configurations demonstrate better performance because of the transitory components on the catalyst surface (Fig. 4). However, the configuration enactment is a function of the catalyst type and VOCs in the gas stream. Both the configurations have the flexibility to load the catalyst within the reactor, especially in a packed bed reactor (PBR) or are positioned only on its surface (Chen et al. 2016; Huang et al., 2010; Saoud et al., 2019; Mei et al. 2016; Li et al. 2015; Jo et al. 2016). However, studies have presented a configuration with an inner electrode covered with a thin TiO_2 film (Subrahmanyam, 2009; Subrahmanyam et al., 2007).

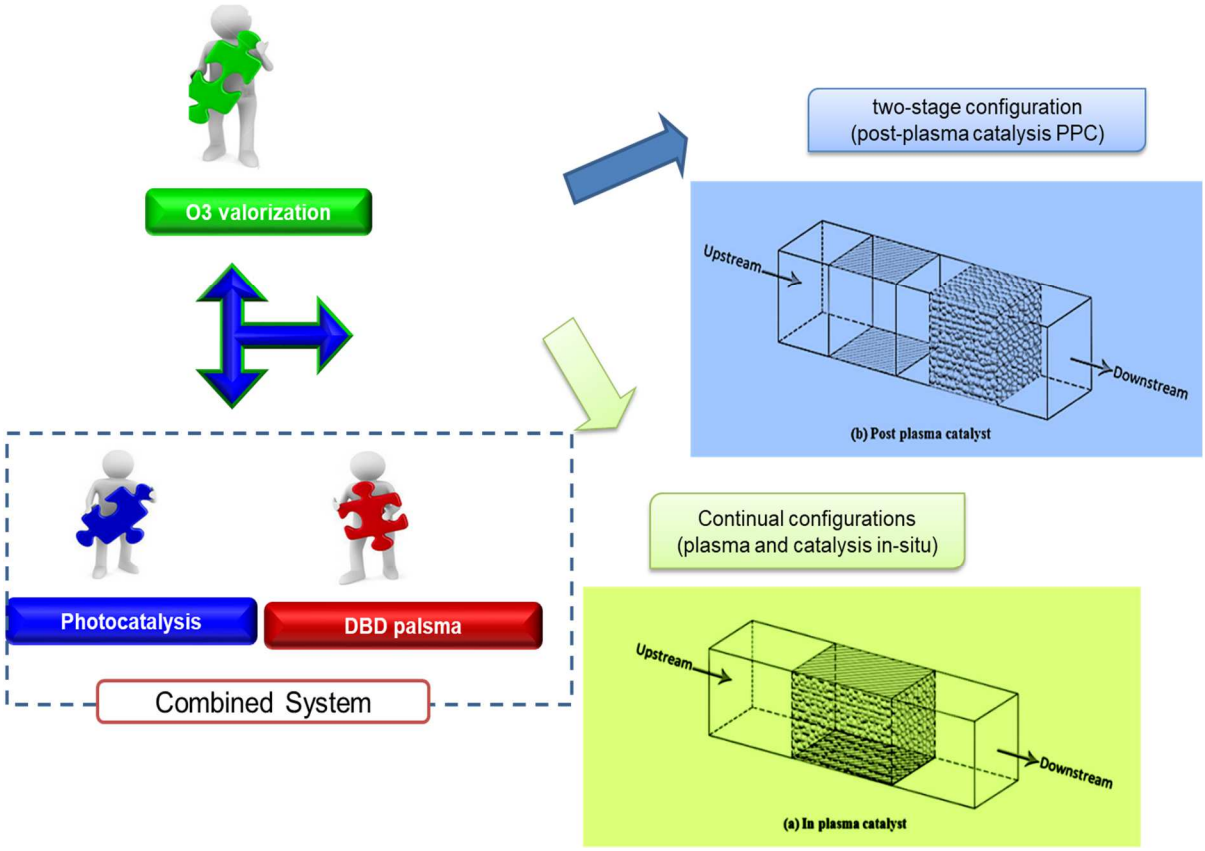

287

288 **Figure 4:** Typical process flow diagrams and description of the main functions of
289 Post Plasma Catalyst (PPC) and In Plasma Catalyst (IPC) system (Assadi, 2012)

290 In most reactor configurations with packed beads, the catalysts are deposited
291 on glass beads, which also play the role of a dielectric barrier of the plasma reactor.
292 Furthermore, TiO_2 can be used in a pure state (Guaitella et al., 2005; Rousseau et
293 al., 2005) or doped on a support such as silica gel (Futamura et al., 2004), Al_2O_3
294 (Kang et al., 2006; Lee et al., 2004) or other porous materials. It is also reported that
295 TiO_2 can be deposited on Ni/Al_2O_3 foam (Huang and Ye, 2009; Huang et al., 2010),
296 activated carbon (Sun et al., 2007; Taranto et al., 2007), and zeolite of ZSM-5
297 monolith and Raschig rings (Annesi-maesano et al., 2011). A powdered form of the
298 catalyst can be used to cover the surface of the reactor (Futamura et al., 2004; Sano
299 et al., 2006). Furthermore, the catalyst can also be doped onto a support such as
300 glass fibers (Guaitella et al., 2008; Thevenet et al., 2008, 2007) or activated carbon

material (Hou and Ku, 2013). It is interesting to note that a block of $TiO_2/Al_2O_3/SiO_2$ placed in the reactor has also been used (Durme et al., 2007), as presented in Table 2. Despite their photocatalytic activity, the porosity of these materials has compelling adsorption capacities

Table 2. Different catalysts used in the combined systems.

Target pollutant	Reactor design	Catalyst and positions	References
Toluene	DBD	Co-MCM-41 (IPC)	(Xu et al., 2016)
	Photocatalytic DBD	TiO_2/SMF (IPC)	(Chen et al., 2016)
	Pulsed DBD	Pd/γ-Al_2O_3 (IPC)	(Huu et al., 2017)
Formaldehyde	Packed bed DBD	$NaNO_2$ (IPC)	(Liang et al., 2010)
	DBD	Cu/CeO_2 (IPC)	(Zhu et al., 2015a.)
	Packed bed DBD	Ag/CeO_2 (IPC)	(Huixian and Zengfeng, 2009)
	Corona discharge	MnO_x/Al_2O_3 (PPC)	(Wan et al., 2011)
Benzene	DBD	TiO_2/MnO_x/SMF (IPC)	(Linga et al., 2014)
	Packed bed DBD	Ag/TiO_2 (IPC)	(Kim et al., 2005)
	Packed bed DBD	Ag0.9Ce0.1/γ-Al_2O_3 (IPC)	(Jiang et al., 2015)
Trichloroethylene	Corona discharge	$Pd/LaMnO_3$ (PPC)	(Vandenbroucke et al., 2016)
	Corona discharge	$CeMn_4$ (PPC)	(Dinh et al., 2015)
	DBD	Au-mesoporous silica (PPC)	(Magureanu et al., 2007)
Propionic acid and benzene	DBD	SiO_2-TiO_2 (IPC)	(Zadi et al., 2020)
Mixture VOCs	DBD	MnO_x/SMF (IPC)	(Ramaraju and Subrahmanyam, 2014)
Mixture VOCs	DBD	AgO_x/MnO_x/SMF (IPC)	(Karuppiah et al., 2013)
Mixture VOCs	Corona discharge	MnO_x/Al_2O_3 (PPC)	(Wan et al., 2011)

4.3 Plasma/photocatalytic operation mode

The plasma DBD reactors combined with photo-catalyst have been tested for the removal of numerous VOCs and NOx. Nonetheless, we are limited in our review to present only the VOCs tested in lab-scale and pilot-scale operations. For instance, the central part of the investigations has been devoted to the habitually available VOCs such as toluene (Jo et al., 2016; Sun et al., 2007), Butadione (Saoud et al., 2020) acetylene (Guaitella et al., 2008), benzene (Futamura et al., 2004; Lee et al., 2004; Zhu et al., 2009), chloroform (Zadi et al., 2020), fatty acids (Zadi et al. 2018) and butyraldehyde (Saoud et al., 2019).

TiO_2 photo-catalyst is typically activated by using UV radiation at wavelengths typically less than 388 nm. This fact requires the arrangement of UV lamps outside the photocatalytic reactors for ensuring uniform illumination and activation of the photo-catalyst (Assadi et al., 2018; Jo et al., 2016; Ramaraju and Subrahmanyam, 2014). The plasma-driven photocatalysis UV light is widely utilized in hybrid plasma-photocatalytic systems (Sivachandiran et al., 2013; Shi et al., 2016; Palau et al., 2015; Subrahmanyam, 2009; Saoud et al., 2018). The ability of plasma radiation for TiO_2 activation is discussed below.

(Rousseau et al., 2005) studied the combination of TiO_2 and a low-pressure plasma discharge to oxid acetylene using a batch reactor. In this study, the authors presented the synergistic interactions between the volumetric plasma discharge and an externally illuminated TiO_2 catalyst. (Thevenet et al., 2008, 2007) studied the elimination of acetylene in a recirculation reactor loaded with a TiO_2/SiO_2 catalyst. The authors reported that the plasma discharge on porous catalytic material results in more CO and oxidized components. Nonetheless, in the presence of an externally illuminated UV lamp, they noted an increase in the acetylene removal potency with an increase in the mineralization efficiency (Thevenet et al., 2008, 2007).

Subsequently, it can be deduced that, regardless of the operational mode, laboratory-scale experiments have shown that a hybrid photocatalytic plasma discharge can increase the elimination performance of VOCs due to the existence of synergistic effects (Thevenet et al., 2008, 2007).

Some key factors that lead to the synergetic effects are mentioned below:

(i) The by-products attached to the photo-catalyst surface (especially TiO_2) can be desorbed using the plasma for mineralization (Assadi et al., 2014c; Ghaida et al., 2016; Palau et al., 2015; Saoud et al., 2019; Zadi et al., 2020).

(ii) TiO_2 activation occurs through the plasma ion bombardment and generation of electron-hole pairs (Assadi et al., 2018, 2014c, 2014b).

(iii) Plasma can generate ionic products, radicals, high-energy electrons to promote the mass transfer of the pollutants from the bulk phase to the solid phase (Ghaida et al., 2016).

5. Plasma discharge and photo-catalyst combination: actives species and reaction mechanism

5.1 Plasma discharge

The electrons formed can collide directly with the existing molecules when a plasma discharge occurs in the air (Annesi-maesano et al., 2011; Visscher et al., 2008; Wang and Chen, 2009). This collision reaction results from different reactions patterns like dissociation or excitation and reactive species (e.g., $O°$, $O_2°^-$ and $N_2°$). While atomic oxygen $O°$ is short-lived for lower than a millisecond (Allegraud, 2009), $N_2°$ and $O_2°$ can be reactive and short-lived for about a few microseconds.

$$O_2 + e^- \rightarrow O° + O° + e^- \qquad (1)$$

357 $$O_2 + e^- \rightarrow O_2^\circ + e^- \quad (2)$$

358 $$N_2 + e^- \rightarrow N_2^\circ + e^- \quad (3)$$

359 It is important to note that these unstable ROS and RNS rapidly undergo
360 reactions for re-institution to their ground states. They could also generate some
361 long-lived species like ozone (Futamura et al., 2004).

362 $$O^\circ + O_2 + M \rightarrow O_3 + M \quad (4)$$

363 $$O_2^{\circ-} + O_2 \rightarrow O_3 + O^\circ \quad (5)$$

364 $$N_2^\circ \rightarrow N_2 + h\gamma \quad (6)$$

365 ROS can degenerate with the generation of intermediate by-products followed by
366 their oxidation. Besides, Eq. (7) illustrates the complete oxidation of a VOC, where
367 the intermediate products are CO and other VOCs with a carbon number less than
368 that in P.

369 $$Pox \rightarrow \ldots \rightarrow : : : ox \rightarrow CO_2 + H_2O \quad (7)$$

370 For conventional VOCs such as the BTEX family (benzene, toluene,
371 ethylbenzene and xylene), the elimination of these pollutants by applying ozone is
372 insignificant in contrast to the oxidation by O° (Zadi et al., 2018). Moreover, cold
373 plasma makes the reaction possible between VOCs and electrons. However, the
374 treatment of acetylene by plasma is insignificant (Rousseau et al., 2005).

375 (Chang and Lin, 2005) reported that a reactor filled with glass beads led to an
376 increase in the removal efficiency of toluene and acetone when compared to that of
377 the empty reactor. Regardless of the residence time due to the glass beads packing

inside the reactor, the formation of plasma on their entire surface efficiently leads to the VOCs denaturation.

The mineralization (CO_2 selectivity) may not result from the use of glass beads. A tenuous rise in the selectivity of CO_2 has been noticed with neutral packing in the case of acetone treatment (Chang and Lin, 2005). It has been suggested that the presence of an oxygen atom in the pollutant structure would promote the formation of CO and CO_2. It should be noted that the plasma can form specific long-lived molecules, such as NO, N_2O, and NO_2, as shown in Eq. (8) to Eq. (12).

$$N_2 + e^- \rightarrow N + N + e^- \quad (8)$$

$$N + O_2 \rightarrow NO + O° \quad (9)$$

$$N + O_3 \rightarrow NO + O_2 \quad (10)$$

$$NO + O_3 \rightarrow NO_2 + O_2 \quad (11)$$

$$NO_2 + O_3 \rightarrow NO_3 + O_2 \quad (12)$$

As shown in Eq. (11) and Eq. (12), a rise in NO_x concentration, as well as that of NO and NO_2 as a result of catalytic reactions, can lead to a reduction in the levels of ozone concentration (Annesi-maesano et al., 2011).

5.2. Plasma and photocatalysis (without external UV light)

An extrinsic UV light illumination on the photocatalytic surface is responsible for the formation of electron-hole pairs. Under these conditions, the material does not have any photo-catalytic activity to participate in the oxidation of the pollutant. Nevertheless, other reactions should not be disregarded that could considerably involve the VOC oxidation process. Under certain conditions, even without being

activated, the photo-catalyst can play the role of an adsorbent of the pollutant present in the gas phase, mainly when carried on porous supports with a very high specific surface area (Guaitella et al., 2005). The pollutant adsorption on the photo-catalyst surface makes it possible to increase its adequate residence time in the reactor, which argues in favour of increasing the pollutant-ROS contact produced by the plasma (Guaitella et al., 2008; Thevenet et al., 2007).

Furthermore, the deposition of the photo-catalyst in the plasma zone (IPC) can lead to oxidation being intervened by the ROS. The short-lived components could recombine before reaching the plasma downstream (PPC) where the catalyst is loaded. Consequently, ROS such as ozone with a relatively long lifetime can react with the pollutant adsorbed on the photo-catalyst surface.

It is well known that the loading of TiO_2 in the discharge zone illuminated with an external UV can increase the generation of ozone at the reactor exhaust. This phenomenon is because TiO_2 furnishes additional surface area in the reactor as indicated in Eq. (4) (Allegraud, 2009).

5.3 Plasma and photocatalysis (with external UV light)

External UV illumination is required outside the reactor to ensure proper activation of TiO_2 for processes involving photocatalysis and cold plasma. As indicated in Eq. (6), plasma discharge could emit photons for activating the photo-catalyst. The energy necessary to yield electron-hole pairs on the photo-catalyst surface could be directly provided by the reaction of nitrogen radical with the photo-catalyst, i.e. $N_2°$ with TiO_2 (Durme et al., 2007). Several authors have proposed that it is theoretically possible to activate TiO_2 by UVs of the plasma (Saoud et al., 2019; Subrahmanyam, 2009; Zadi et al., 2018). Some studies suggest that the activation by

an external UV lamp generates important photocatalytic activities (Jo et al., 2016; Subrahmanyam, 2009; Subrahmanyam et al., 2007; Sun et al., 2007; Zhu et al., 2009), while a few other studies suggest otherwise (Bao et al., 2007; Futamura et al., 2004; Guaitella et al., 2008; Rousseau et al., 2005; Sano et al., 2006; Thevenet et al., 2007). It is, therefore, ambiguous to ascertain the reason for these paradoxical results.

It should be noted that after the activation of the photo-catalyst by an external UV light source, the reactions independent of light are also conceivable during the plasma discharge. Moreover, an external source of UV light could also lead to photolysis to denature the adsorbed VOCs and ozone into ROS provided the emitted radiation has a wavelength of 200-308 nm, as indicated in Eq. (13) (Huang and Ye, 2009).

$$O_3 + h\nu \rightarrow O_2 + O^\circ \qquad (13)$$

As mentioned previously, the generation of electron-hole pairs on the photo-catalyst surface area is due to the irradiation of the photo-catalyst. Subsequently, along with the photo-catalyst, the electron-hole pairs and the species produced by the plasma discharge react with the adsorbed pollutant leading to its denaturation. Atomic oxygen is a resilient oxidizing agent responsible for VOC decomposition (Durme et al., 2008; Ghaida et al., 2016; Subrahmanyam et al., 2010; Trinh and Mok, 2015; Visscher et al., 2008). It is produced by the degradation of ozone adsorbed on the photo-catalyst surface (TiO_2). This synergistic effect is evident with the association of plasma discharge, a suitable photo-catalyst, and an external UV illumination, preferably in an IPC configuration (Assadi et al., 2014b; Saoud et al., 2017; Zadi et al., 2018). This result indicated that the effectiveness of pollutant

degradation by an individual process is relatively lower than that of the hybrid process (Assadi et al., 2017; Saoud et al., 2017; Zadi et al., 2020).

$$O_{3\,(ads)} + e^{-} \rightarrow O^{\circ} + O_2 \qquad (14)$$

As previously mentioned in Eq. (14), the ozone decomposition on the photo-catalyst surface aids in the decay of its residual concentration in a hybrid process involving plasma discharge and the UV-activated photo-catalyst. Besides, the pollutant removal rate increase is observed because of the O° species reaction with the adsorbed VOCs (Assadi et al., 2014b; Saoud et al., 2017; Zadi et al., 2020). Since the only reactive component inside the photocatalytic zone is ozone, PPC reactors make the former reaction more apparent. In contrast, plasma discharge in the IPC reactors facilitate the formation of short-lived species in its photocatalytic zone. In the next step, the short-lived species are adsorbed on the surface of the photo-catalyst for selective reaction with pollutants present in the gas phase (Durme et al., 2007). Such type of reactor configurations makes ozone dissociation relatively insignificant (Fig. 5).

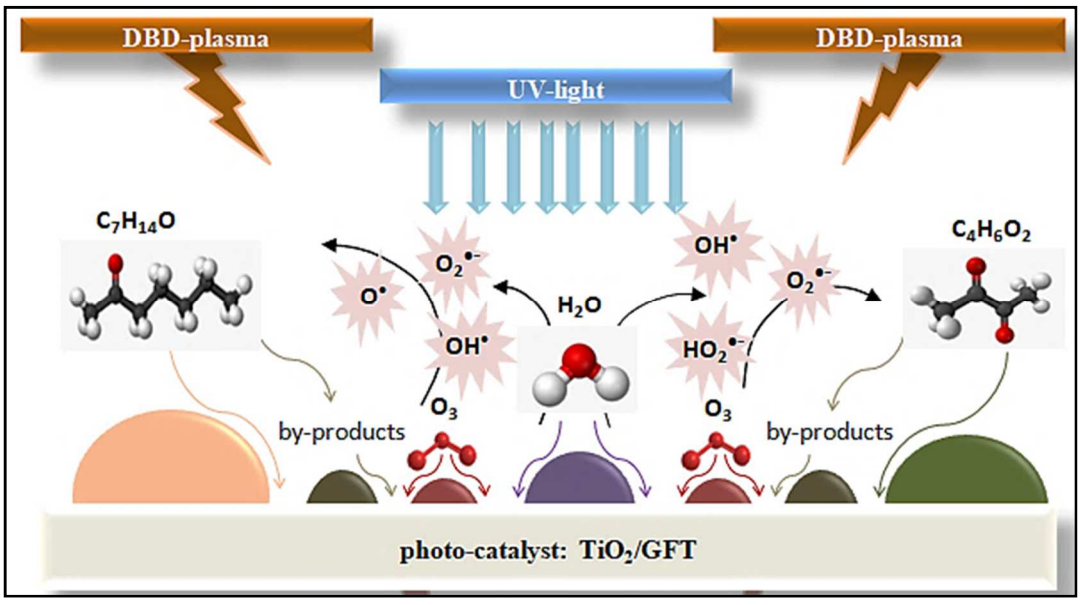

Figure 5. A suggested mechanism for ROS interaction with pollutants under simultaneous DBD-plasma/photocatalysis (TiO2 deposed on glass fiber tissue (GFT)) (Saoud et al., 2020).

The coupling of plasma discharge and the photo-catalyst could favor both the conversion/decomposition of the pollutant and the mineralization of the by-products compared to each process performed separately (Futamura et al., 2004; Guaitella et al., 2008; Lee et al., 2004; Saoud et al., 2018, 2017; Subrahmanyam, 2009). For example, a packed bed of TiO_2, in the post-discharge zone, conducts more significant mineralization than any packing material of a similar size (Chang and Lin, 2005). Hence, a photo-catalyst is responsible for mineralization instead of–porous material. The hybrid process also reduces the type and amount of intermediate degradation products and by-products (Sun et al., 2007).

Some authors have confirmed that plasma has an appealing impact on photo-catalyst life. TiO_2 is gradually poisoned in the photocatalysis process alone (Futamura et al., 2004). This fact is because of the non-reversible adsorption of HNO_3 (Durme et al., 2007) and H_2SO_4 (Portela et al., 2007). A plasma discharge can regenerate the photocatalytic activity by uptaking a portion of the compounds (e.g., sulfur-containing species) responsible for the poisoning of photo-catalyst and loss of its effectiveness (Futamura et al., 2004; Huang and Ye, 2009; Sun et al., 2007).

6. Effect of some key parameters on VOCs removal efficiency

6.1 Relative Humidity (RH) effect

We note that all the mechanisms mentioned above are compatible with plasma DBD beneath dry air. Nevertheless, the water molecule is naturally accompanying pollutants in the air. Water vapour present in the system alters the ROS and RNS resulting from plasma discharge substantially. This phenomenon

happens when it reacts with the electrons liberated from plasma discharge or with some active species (D.P. Subedi, U.M. Joshi, 2017) originating from the photocatalytic reactions (Abidi et al., 2020; Saoud et al., 2020).

$$H_2O + e^- \rightarrow H^\circ + HO^\circ + e^- \quad (15)$$

$$H_2O + O^\circ \rightarrow HO^\circ + HO^\circ \quad (16)$$

$$H_2O + N_2^\circ \rightarrow N_2^\circ + OH^\circ + H^\circ \quad (17)$$

$$H_2O_{ads} + h^+ \rightarrow HO^\circ_{ads} + H^+_{ads} \quad (18)$$

It should be noticed that the HO° radical produced by the above reactions is a more potent oxidant than those investigated so far (Portela et al., 2007). For example, the kinetic constant of toluene oxidation by HO° is greater than that by O°. Hence, the degradation aided by ozone is trivial compared to that with HO° radicals (Durme et al., 2007; Maxime and Amine, 2014). Besides, HO° also stabiles the activity of a photo-catalyst by decelerating its deactivation (Thevenet et al., 2008). Even if humidity considerably increased the efficiency of plasma photocatalysis, few studies have shown adverse effects. On the one hand, studies proposed that it reduces the discharge in the case of gas-phase release. Thus, the energy and concentration of the electrons, then the ROS formed by the plasma (D.P. Subedi, U.M. Joshi, 2017; Durme et al., 2007; Ye and Tian, 2006). Besides, upon its adsorption at higher amounts, it can create a layer preventing the access to pollutants and reagents, thus reducing the efficacy of pollutant decomposition by the photo-catalyst (D.P. Subedi, U.M. Joshi, 2017; Durme et al., 2007).

Relative humidity of the gas phase can influence the degradation of pollutants and the harmful effects associated with the recombination of free radicals. However,

this depends mainly on the operating conditions, such as the co-concentration of the contaminent. The occurrence of HO° radicals depends on the concentration of water in the reaction; hence, the degradation rate of pollutants can rise with the concentration of water (Huang and Ye, 2009). In contrast, an increase in the relative humidity is found to lower the rate of pollutant conversion or decomposition regardless of the coupling configuration (i.e., IPC or PPC type reactors) (Durme et al., 2007; Thevenet et al., 2008). Some studies have confirmed that HO° radicals promote the conversion of CO into CO_2, thus leading to a higher mineralization rate at greater water concentrations (Kim et al., 2015; Ye and Tian, 2006). However, an inadequate fraction of water can inhibit the photo-catalyst, thereby reducing its selectivity for CO_2 mineralization (Huang and Ye, 2009).

The existence of water vapor, particularly in PPC reactors, can reduce ozone emissions at the reactor outlet (Durme et al., 2007). However, the same study (Durme et al., 2007) reported that, at a humidity below 30%, the ozone concentration is unaffected in the IPC system compared to the configuration of plasma alone. Besides, they have shown that humidity diminishes the emanation of NO_2 and, afterword, raises the catalyst service life (Durme et al., 2007).

6.2 Effect of the applied voltage

Increasing the input energy density can lead to an increase in the discharge of the plasma and a rise in the concentration of released electrons and their corresponding energies (Lu et al., 2014). Subsequently, more collisions occur with the other species/pollutants existing. Consequently, the concentrations of ROS, like the radicals O° and HO°, are also increased, principally in charge of the degradation and mineralization of pollutants (Costa et al., 2016; Visscher et al., 2008). Therefore,

it is compelling to indicate that the feeding energy density is not affected by the association of plasma discharge and a photo-catalyst under steady process parameters (Bao et al., 2007; Chang and Lin, 2005; Durme et al., 2007; Futamura et al., 2004; Guaitella et al., 2008; Huang et al., 2010; Subrahmanyam, 2009; Zhu et al., 2009). Nonetheless, CO_2 selectivity can elevate with amplification in energy density (Futamura et al., 2004; Lee et al., 2004; Maxime and Amine, 2014; Sano et al., 2006; Subrahmanyam, 2009; Subrahmanyam et al., 2007). Additionally, it should be mentioned that the concentrations of ozone (Bao et al., 2007; Durme et al., 2007; Huang and Ye, 2009; Huang et al., 2010; Maxime and Amine, 2014) and NO_2 (Durme et al., 2007), at the reactor exit behave proportionally as well as the input energy. Thus, an optimal feeding energy density and an appropriate photo-catalyst are essential to enhance the pollutant decomposition and reduce the concentrations of ozone and NO_x at the reactor outlet.

6.3 Other significant parameters

Table 3 summarizes the different effects of other keys parameters on plasma combined with photocatalysis.

Table 3. Impacts of widely studied parameters for the decomposition of pollutants in the hybrid plasma-photocatalytic process

	Flow rate	**Pollutant concentration**	**Amount of photo-catalyst**	**Level of oxygen in the gas phase**
Elimination efficiency Selectivity of CO_2	(-) (D.P. Subedi, U.M. Joshi, 2017; Thevenet et	(-) (D.P. Subedi, U.M. Joshi,	(+) (Monteiro et al., 2015)	(-/+) Optimum 1-5% (D.P. Subedi, U.M. Joshi, 2017)

al., 2014) 2017)

As shown in Table 3, increasing the effluent gas flow and the concentration of pollutants decreases the elimination efficacy and the CO_2 selectivity. Therefore, more research is necessary for optimizing process parameters and operating conditions.

As explained previously, a hybrid of the plasma and photocatalytic processes can surpass the efficacy of the two processes assessed individually. The coupling of both processes has many synergistic effects.

Coupling both the processes promotes pollutant decomposition and mineralization while diminishing the chances of undesirable by-product formation. Such mechanisms remain less understood; hence the inferences from various studies available in the literature in certain aspects are contradictory owing to a wide variety of the investigated systems and the involved process variables.

Owing to these reasons, the comparison of the reactors performance considered in proportion to their configurations is not possible, which given their great diversity, would have been interesting. Nevertheless, coupling plasma and photocatalytic processes seem to be promising, except for the deficiency of available data in the literature~~,~~ concerning pollutants other than VOCs.

7. Hybrid plasma/photo-catalytic reactor design

Traditionally, the studies concerning dielectric barrier discharges involved inserting materials (e.g., $BaTiO_3$) having a high relative permittivity into the plasma discharge zone to enhance their electrical properties. The electric field at the circumference is strengthened through micro-discharges upon the particles of matter

polarization at the plasma discharge zone. (Ray and Subrahmanyam, 2016) have proposed that the properties of the material incorporated into the plasma reactor enhance both the pollutant decomposition and the selectivity of CO_2. The changes also influence the increased effectiveness of the plasma reactor in the operating conditions leading to plasma discharge and material characteristics. A coaxial cylindrical reactor is a commonly used reactor, both in the laboratory- and industrial-scale processes. This characteristic is a type of PBR reactor in which the discharge space is packed with pellets of catalysts (Assadi, 2012).

(Holzer et al., 2002) have studied the oxidation of VOCs using an amalgamation of heterogeneous catalysis and non-thermal plasma discharge. The study demonstrated the benefits of adding a porous material with non-photocatalytic activity to a dielectric barrier discharge. The accessibility of short-lived active components generated from plasma discharge was feasible because of their diffusion into the porous structure of σ-alumina and silica gel. Introduction of photocatalytic materials (e.g., TiO_2, ZnO, and SnO_2) in the plasma discharges can offer several benefits of the higher specific surface area and potentially reactive compounds (Holzer et al., 2002; Li et al., 2001). (Li et al., 2001) observed that TiO_2 addition into a corona discharge considerably enhanced toluene denaturation. The authors suggested a possible surface activation by the active component. However, the approach of photocatalytic activation by UV rays generated in the corona discharge is required to be well understood.

(Kang et al., 2002) reported a transition in the decomposition rate for toluene under a pulsed oxygen discharge from 40% to 70%. This result was possible upon loading TiO_2 on a glass substrate through a sol-gel technique for a plasma discharge. The authors also reported that the rise in the pollutant conversion rate is a function of

601 the voltage employed to each pulse. However, the interaction between the two
602 processes is not well understood.

603 Some notable findings of the hybrid plasma/photocatalytic processes for VOC
604 removal are summarized in Table 4. (Andersen et al., 2013) reported eliminating
605 methanol, styrene, and butyl acetate in the shale oil treatment plant exhausts and a
606 hull production site. They observed nearly 71% and 74% decomposition of butyl
607 acetate, methanol, and styrene under specific input energy (SIE) of 220 and 300 J/L,
608 respectively (Andersen et al., 2013). Some field tests have been carried out for spice
609 plants and rubber with a prototype plasma deodorant intended for remedying a gas
610 flow up to 10 m^3/min (Mizuno, 2007). The efficiency of gas deodorization was
611 quantified by odours concentration utilizing an olfactive measurement method. The
612 elimination efficiency of toluene at a level of 10 ppm in the ambient air and a catalytic
613 combustion system assisted by plasma reached almost 90% with a gas flow rate of
614 60 m^3/min. (Beckers et al., 2013) investigated the denaturation of H_2S, NH_3, NO_x,
615 limonene, toluene, along with the elimination of fine dust particles in a semi-industrial
616 scale facility using a pulsed corona system. The system demonstrated the feasibility
617 of air purification on a large scale as the efficiency reaches 90-100% for all the tested
618 target pollutants.

619 Different technologies are commonly used that can produce corona discharge
620 (plasma generated by electrical discharges) (Beckers et al., 2013), dielectric barrier
621 discharge (Martin et al., 2008; Murali et al., 2019), and non-thermal plasma. An
622 amalgamation of photocatalysis and plasma discharge can provide high treatment
623 performance with many synergistic effects (Assadi et al., 2015, 2014a; Dou et al.,
624 2016; Mei et al., 2016; Murali et al., 2019). As illustrated in Fig. 6 the pilot-scale

reactor can operate solely as a DBD plasma system and photocatalytic system or as a hybrid system (photocatalysis coupled with DBD plasma).

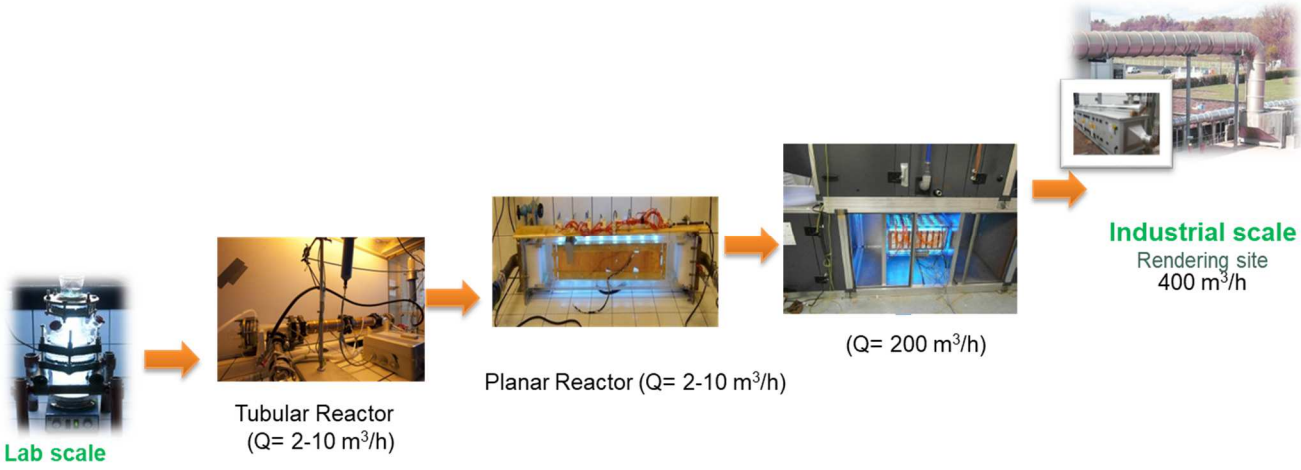

Figure 6. Industrial pilot combining plasma and in situ photocatalysis.

The coupled reactor configurations illustrated by (Martin et al., 2008) have the following advantages:

(i) pollutant oxidation facilitated by ions and free radicals generated by the activated species under a dielectric barrier discharge, and

(ii) pollutants/by-products adsorption on a mineral bed.

Table 4. Pollutant removal with photocatalytic-plasma oxidation on an industrial scale.

Reactor configuration	Pollutant	Operating condition	Catalysts	performance	Ref.
Corona discharge reactor	Indole	Concentration of pollutant: 2 ppb Flow rate: 45 and 70 m^3/h	None	90% for both pollutants	(Andersen et al., 2013)
Pulsed corona	Toluene	Concentration: 10 ppm Flow rate: 60 m^3/min	Zeolite	90% of toluene	(Mizuno, 2007)

discharge					
Pulsed corona discharge	NH_3, H_2S, limonene, and fine dust	Concentration:15-70 ppm Flow rate: 150-528 m^3/h	None	90% of NO_x 90-100% of toluene, limonene, H_2S and fine dust	(Beckers et al., 2013)
Dielectric Barrier Discharge (DBD)	Isobutyraldehyde, isovaleraldehyde	Concentration:30 mg/m Flow rate: 250 m^3/h	Glass Fiber Tissue	60-75% for the three aldehydes	(Murali et al., 2019)
Dielectric Barrier Discharge (DBD)	Naphthenic and paraffinic bitumen fume	Flow rate: 40-50 m^3/h	Adsorbent (Mineral filters)	Complete removal	(Martin et al., 2008)
Corona discharge	Toluene	Concentration: 8.2–1000 ppbv Flow rate: 3-9 m^3/h	None	98.2% at 8.2 ppbv	(Ondarts et al., 2016)
DBD surface discharge	Acetone and toluene	Concentration: 0.2 ppm Flow rate : 38.42 m^3/h	Pt/TiO_2 and $MnO_2/CuO_2/Al_2O_3$	100% toluene and acetone abatement with 0.2 ppm and 0.46 ppm, respectively.	(Jia et al., 2015)
Dielectric Barrier Discharge (DBD)	Butyl acetate, styrene, and methanol	Concentration:30-110 ppm Flow rate: 2.5 and 5 m^3/h	None	71% of butyl acetate 74% of styrene and methanol	(Schmidt and Jo, 2015)

GlidArc discharge	TNT, o-xylene sarin	Concentration:160 ppm; 1,38 ng/m^3 (of TNT/Sarin) Flow rate : up to 200 m^3/h	None	81,25% at 160 ppm 97% at 1,38 ng.m^{-3}	(Czernichowski and Czernichowski, 2009)

8.Practical applications and future research prospects

Among the gas phase processes, there are promising zero waste & zero reagent technologies such as the coupling between dielectric barrier discharge plasma (DBD) and catalysis. These processes are very interesting prospects in terms of synergy, with low energy consumption. However, the by-products are reduced with the plasma coupling and photo-catalyst, the quantity of NOx and ozone at the outlet of the reactors remains non-negligible. All of these present a significant challenge requiring more investigations to be conducted within the framework of a post-discharge treatment.

9. Conclusions

In this review, for each operating condition and tested key parameter, a synergetic effect could be observed at the laboratory, and pilot scales were unambiguously confirmed. Based on the review of available literature, the combined photocatalysis and plasma processes can present an improved efficiency for pollutant reduction compared to their functionalities realized individually. The enhancement in performance can be to (i) the scavenging of plasma active species by catalytic surface (ii) surface regeneration with discharge (iii) ozone decomposition with UV radiation. From our point of view, the expenditures associated with VOC treatment can be ,mitigated by applying cutting-edge technologies.

10. Acknowledgments:

This work was supported by the King Khalid University, Abha, Saudi Arabia (by grant R.G.P. 1/257/42). We express our gratitude to the Deanship of Scientific Research, King Khalid University, for its support of this study. The authors thank the ENSCR, Université du Québec à Trois-Rivieres (UQTR), Canada and Kyonggi University, Korea, for their scientific collaboration.

11. References

Abidi, M., Hajjaji, A., Bouzaza, A., Trablesi, K., Makhlouf, H., Rtimi, S., Assadi, A.A., Bessais, B., 2020. Simultaneous removal of bacteria and volatile organic compounds on Cu2O-NPs decorated TiO2 nanotubes Competition effect and kinetic studies Journal of Photochemistry & Photobiology A : Chemistry Simultaneous removal of bacteria and volatile organic compounds on Cu 2 O- NPs decorated TiO2 nanotubes : Competition e ff ect and kinetic studies. J. Photochem. Photobiol. A Chem. 400, 112722. https://doi.org/10.1016/j.jphotochem.2020.112722

Allegraud, K., 2009. Décharge à Barrière Diélectrique de Surface : Physique et procédé Katia Allegraud To cite this version : HAL Id : pastel-00004783 Décharge à Barrière Diélectrique de surface : physique et procédé Laboratoire de physique et technologie des plasmas.

Alonso-tellez, A., Robert, D., Keller, V., Keller, N., 2014. H2S photocatalytic oxidation over WO3/TiO2 Hombikat UV100. Environ. Sci. Pollut. Res. 3503–3514. https://doi.org/10.1007/s11356-013-2329-y

Almomani F., R. Rene E., Veiga M. C., Bhosale R. R., Kennes Ch., 2021, Treatment of waste gas contaminated with dichloromethane using photocatalytic oxidation, biodegradation and their combinations, Journal of Hazardous Materials, 405, 123735, https://doi.org/10.1016/j.jhazmat.2020.123735

Almomani F, Bhosale R, Shawaqfah M, 2020, Solar oxidation of toluene over Co doped nano-catalyst, Chemosphere, 255, 126878 https://doi.org/10.1016/j.chemosphere.2020.126878.

Andersen, K.B., Beukes, J.A., Feilberg, A., 2013. Non-thermal plasma for odour reduction from pig houses – A pilot scale investigation. Chem. Eng. J. 223, 638–646. https://doi.org/10.1016/j.cej.2013.02.106

690 Andryushina, N.S., Stroyuk, O.L., 2014. Environmental Influence of colloidal graphene oxide
691 on photocatalytic activity of nanocrystalline TiO 2 in gas-phase ethanol and benzene
692 oxidation. Applied Catal. B, Environ. 148–149, 543–549.
693 https://doi.org/10.1016/j.apcatb.2013.11.044
694 Annesi-maesano, I., Behalf, O.N., The, O.F., Study, G., 2011. Estimating the Health Effects
695 of Exposure to Multi-Pollutant Mixture. https://doi.org/10.1016/j.annepidem.2011.11.004
696 Assadi, A., Bouzaza, A., Wolbert, D., 2012. Chemistry Photocatalytic oxidation of
697 trimethylamine and isovaleraldehyde in an annular reactor : Influence of the mass
698 transfer and the relative humidity. Journal Photochem. Photobiol. A Chem. 236, 61–69.
699 https://doi.org/10.1016/j.jphotochem.2012.03.020
700 Assadi, A.A., 2012. Développement d'un procédé de couplage réacteur plasma DBD-
701 réacteur photocatalytique pour le traitement des effluents gazeux : du laboratoire à
702 l'application industrielle. thèse ENSCR n °9.
703 Assadi, A.A., Bouzaza, A., Penya-roja, J., Martinez-soriac, V., Wolbert, D., Assadi, A.A.,
704 Bouzaza, A., Penya-roja, J., Martinez-soriac, V., 2014a. Abatement of 3-methylbutanal
705 and trimethylamine with combined plasma and photocatalysis in a continuous planar
706 reactor To cite this version : HAL Id : hal-00981617.
707 Assadi, A.A., Bouzaza, A., Soutrel, I., Petit, P., Medimagh, K., Wolbert, D., Assadi, A.A.,
708 Bouzaza, A., Soutrel, I., Petit, P., Medimagh, K., 2017. A study of pollution removal in
709 exhaust gases from animal quartering centers by combining photocatalysis with surface
710 discharge plasma : From pilot to industrial scale To cite this version : HAL Id : hal-
711 01475458. Chem. Eng. Process. Process Intensif.
712 https://doi.org/10.1016/j.cep.2016.10.001
713 Assadi, A.A., Bouzaza, A., Wolbert, D., 2014b. Use of DBD plasma, photocatalysis, and
714 combined DBD plasma/photocatalysis in a continuous annular reactor for
715 isovaleraldehyde elimination - Synergetic effect and by-products identification.
716 Assadi, A.A., Bouzaza, A., Wolbert, D., Assadi, A.A., Bouzaza, A., Wolbert, D., 2015. Study
717 of synergetic effect by surface discharge plasma / TiO2 combination for indoor air
718 treatment : sequential and continuous configurations at pilot scale To cite this version :
719 HAL Id : hal-01158449.
720 Assadi, A.A., Bouzaza, A., Wolbert, D., Petit, P., 2014c. Isovaleraldehyde elimination by UV /
721 TiO 2 photocatalysis : comparative study of the process at different reactors
722 configurations and scales 11178–11188. https://doi.org/10.1007/s11356-014-2603-7
723 Assadi, A.A., Loganathan, S., Tri, P.N., Ghaida, G., Bouzaza, A., Tuan, A.N., 2018. Pilot
724 scale degradation of mono and multi volatile organic compounds by surface discharge
725 plasma/TiO reactor Investigation of competition and synergism. J. Hazard. Mater.
726 https://doi.org/10.1016/j.jhazmat.2018.06.007

727 Bao, H., Dai, H.Æ., Ye, Q., Li, Æ.M., Fa, F.Æ., Feng, D., 2007. Contribution of UV light to the
728 decomposition of toluene in dielectric barrier discharge plasma / photocatalysis system
729 577–588. https://doi.org/10.1007/s11090-007-9085-z
730 Beckers, F.J.C.M., Hoeben, W.F.L.M., Huiskamp, T., Pemen, A.J.M., Heesch, E.J.M. van,
731 2013. Pulsed Corona Demonstrator for Semi-Industrial Scale Air Purification. Trans.
732 Plasma Sci. 41, 2920–2925.
733 Boyjoo Y., Sun H. , Liu J., Pareek V. K., Wang S., 2017. A review on photocatalysis for air
734 treatment: From catalyst development to reactor design. Chem. Eng. J. 537-559
735 Bahria M., Haghighata F., Rohanib S., Kazemian H., 2016. Impact of design parameters on
736 the performance of non-thermal plasma air purification system. Chem. Eng. J. 204- 212
737 Chen, J., Xie, Z., Tang, J., Zhou, J., Lu, X., Zhao, H., 2016. Oxidation of toluene by dielectric
738 barrier discharge with photo-catalytic electrode. Chem. Eng. J. 284, 166–173.
739 https://doi.org/10.1016/j.cej.2015.09.006
740 Chuang, L., Luo, C., 2013. Characterization of supported TiO 2 -based catalysts green-
741 prepared and employed for photodegradation of malodorous DMDS. Mater. Res. Bull.
742 48, 238–244. https://doi.org/10.1016/j.materresbull.2012.10.051
743 Costa, G., Assadi, A.A., Ghaida, S.G., Wolbert, D., 2016. Study of butyraldehyde
744 degradation and by-products formation by simulation of relative humidity effect. Chem.
745 Eng. J. https://doi.org/10.1016/j.cej.2016.07.099
746 Czernichowski, A., Czernichowski, P., 2009. GlidArc-assisted cleaning of flue gas from
747 conventional or chemical weapons destructio n 31.
748 D.P. Subedi, U.M. Joshi, C.S.W., 2017. Dielectric Barrier Discharge (DBD) Plasmas and
749 Their Applications. Plasma Science and Technology for Emerging Economies.
750 Dinh, M.T.N., Giraudon, J., Vandenbroucke, A.M., Morent, R., Geyter, N. De, Lamonier, J.,
751 2015. Post plasma-catalysis for total oxidation of trichloroethylene over Ce-Mn based
752 oxides synthesized by a modified “ redox- precipitation route .” Elsevier B.V.
753 https://doi.org/10.1016/j.apcatb.2015.02.013
754 Dou, B., Liu, D., Zhang, Q., Zhao, R., Hao, Q., Bin, F., Cao, J., 2016. Enhanced removal of
755 toluene by dielectric barrier discharge coupling with Cu- Enhanced removal of toluene
756 by dielectric barrier discharge coupling. Catal. Commun. 92, 15–18.
757 https://doi.org/10.1016/j.catcom.2016.12.024
758 Durme, J. Van, Dewulf, J., Leys, C., Langenhove, H. Van, 2008. Combining non-thermal
759 plasma with heterogeneous catalysis in waste gas treatment : A review 78, 324–333.
760 https://doi.org/10.1016/j.apcatb.2007.09.035
761 Durme, J. Van, Dewulf, J., Sysmans, W., Leys, C., Langenhove, H. Van, 2007. Efficient
762 toluene abatement in indoor air by a plasma catalytic hybrid system 74, 161–169.

https://doi.org/10.1016/j.apcatb.2007.02.006

Futamura, S., Einaga, H., Kabashima, H., Yong, L., 2004. Synergistic effect of silent discharge plasma and catalysts on benzene decomposition 89, 89–95. https://doi.org/10.1016/j.cattod.2003.11.014

Elfalleh W., Assadi A.A., Bouzaza A., Wolbert D., Kiwi J., S. Rtimi,2017, Innovative and stable TiO2 supported catalytic surfaces removing aldehydes under UV-light irradiation, Journal of Photochemistry and Photobiology A: Chemistry, 343, 96-102, https://doi.org/10.1016/j.jphotochem.2017.04.029.

Feng, F., Zheng, Y., Shen, X., Zheng, Q.,Dai, S., Zhang, X., Huang, Y., Liu, Z.,Yan, K., 2015. Characteristics of Back Corona Discharge in a Honeycomb Catalyst and Its Application for Treatment of Volatile Organic Compounds, Environ. Sci. Technol., 49, 11, 6831-6837, https://doi.org/10.1021/acs.est.5b00447.

Ghaida, S.G., Assadi, A.A., Costa, G., Bouzaza, A., Wolbert, D., Ghaida, S.G., Assadi, A.A., Costa, G., Bouzaza, A., 2016. Association of surface dielectric barrier discharge and photocatalysis in continuous reactor at pilot scale : butyraldehyde oxidation , by-products identification and ozone valorization To cite this version : HAL Id : hal-01274114.

Guaitella, O., 2010. Nature de la synergie plasma-photocatalyseur pour la destruction d ' un composé organique volatil type : l ' acétylène . To cite this version : HAL Id : pastel-00002918 Nature de la synergie plasma-photocatalyseur pour la destruction d ' un composé organique volatil type : l ' acétylène.

Tong, R., 2019. Emission characteristics and probabilistic health risk of volatile organic compounds from solvents in wooden furniture manufacturing, Journal of Cleaner Production, 208, 1096-1108. https://doi.org/10.1016/j.jclepro.2018.10.195.

Guaitella, O., Gatilova, L., Rousseau, A., 2005. Plasma-photocatalyst interaction : Production of oxygen atoms in a low pressure discharge Plasma-photocatalyst interaction : Production of oxygen atoms in a low pressure discharge 3–6. https://doi.org/10.1063/1.1900314.

Guaitella, O., Thevenet, F., Puzenat, E., Guillard, C., Rousseau, A., 2008. C2H2 oxidation by plasma / TiO2 combination : Influence of the porosity , and photocatalytic mechanisms under plasma exposure 80, 296–305. https://doi.org/10.1016/j.apcatb.2007.11.032.

Han, Z., Chang, V., Wang, X., Lim, T., 2013. Experimental study on visible-light induced photocatalytic oxidation of gaseous formaldehyde by polyester fiber supported photo-catalysts. Chem. Eng. J. 9–18.

Holzer, F., Roland, U., Kopinke, F., 2002. Combination of non-thermal plasma and heterogeneous catalysis for oxidation of volatile organic compounds Part 1 . Accessibility of the intra-particle volume 38, 163–181.

800 Hou, W., Ku, Y., 2013. Chemical Photocatalytic decomposition of gaseous isopropanol in a
801 tubular optical fiber reactor under periodic UV-LED illumination. """Journal Mol. Catal. A,
802 Chem. 374–375, 7–11. https://doi.org/10.1016/j.molcata.2013.03.016.
803 Hu, Y., Song, X., Jiang, S., Wei, C., 2015. Enhanced photocatalytic activity of Pt-doped TiO 2
804 for NO x oxidation both under UV and visible light irradiation : A synergistic effect of
805 lattice Pt 4 + and surface PtO. Chem. Eng. J. 274, 102–112.
806 https://doi.org/10.1016/j.cej.2015.03.135.
807 Huang, H., Ye, D., 2009. Combination of photocatalysis downstream the non-thermal plasma
808 reactor for oxidation of gas-phase toluene 171, 535–541.
809 https://doi.org/10.1016/j.jhazmat.2009.06.033
810 Huang, H.B., Ye, D.Q., Leung, D.Y.C., 2010. Removal of Toluene Using UV-Irradiated and
811 Nonthermal Plasma – Driven Photocatalyst System 1231–1236.
812 Huixian, D., Zengfeng, Z., 2009. Plasma-catalytic removal of formaldehyde in atmospheric
813 pressure gas streams.
814 Huu, T.P., Da, L.S.P., Khacef, C.A., 2017. Methane , Propene and Toluene Oxidation by
815 Plasma-Pd / c -Al 2 O 3 Hybrid Reactor : Investigation of a Synergetic Effect. Top. Catal.
816 60, 326–332. https://doi.org/10.1007/s11244-016-0619-6.
817 Jia, Z., Barakat, C., Dong, B., Rousseau, A., 2015. VOCs Destruction by Plasma Catalyst
818 Coupling Using AL-KO PURE Air Purifier on Industrial Scale 19–26.
819 Jiang, N., Jiang, N., Hu, J., Li, J., Shang, K., Lu, N., Wu, Y., 2015. Plasma-catalytic
820 degradation of benzene over Ag-Ce bimetallic oxide catalysts using hybrid surface /
821 packed-bed discharge plasmas Applied Catalysis B : Environmental Plasma-catalytic
822 degradation of benzene over Ag – Ce bimetallic oxide catalysts using hybrid surface /
823 packed-bed discharge plasmas. https://doi.org/10.1016/j.apcatb.2015.11.044.
824 Jiang, N., Qiu, C., Guo, L., Shang, K., 2017. Post Plasma-Catalysis of Low Concentration
825 VOC Over Alumina-Supported Silver Catalysts in a Surface / Packed-Bed Hybrid
826 Discharge Reactor. https://doi.org/10.1007/s11270-017-3296-6.
827 Jo, J., Quang, T., Kim, S.H., Sun, Y., 2016. Simultaneous removal of hydrocarbon and CO
828 using a non-thermal plasma-catalytic hybrid reactor system. Chem. Eng. J. 299, 93–
829 103. https://doi.org/10.1016/j.cej.2016.04.070.
830 Kang, H., Choi, B., Son, G., Foster, D.E., 2006. C2H4 Decomposition Behavior of a Non-
831 Thermal Plasma Discharge-Photocatalyst System for an Air Purifying Device 49, 419–
832 425.
833 Kang, M., Kim, Bum-joon, Cho, S.M., Chung, C., Kim, Byung-woo, Han, G.Y., Yoon, K.J.,
834 2002. Decomposition of toluene using an atmospheric pressure plasma / TiO 2 catalytic
835 system 180, 125–132.
836 Karuppiah, J., Reddy, E.L., Kumar, P.M., Ramaraju, B., Karvembu, R., Subrahmanyam, C.,

837 2013. Abatement of mixture of volatile organic compounds (VOCs) in a catalytic non-
838 thermal plasma reactor. J. Hazard. Mater. 237–238, 283–289.
839 https://doi.org/10.1016/j.jhazmat.2012.08.040.
840 Karuppiah J., Reddy E.L., Reddy P.M.K., Ramaraju B., Subrahmanyam C., « Catalytic non-
841 thermal plasma reactor for the abatement of low concentrations of benzene ».
842 International Journal of Environmental Science and Technology (2014) 311-318.
843 Kim, H., Oh, S., Ogata, A., Futamura, S., 2005. Decomposition of gas-phase benzene using
844 plasma-driven catalyst (PDC) reactor packed with Ag / TiO 2 catalyst 56, 213–220.
845 https://doi.org/10.1016/j.apcatb.2004.09.008.
846 Kim, H., Teramoto, Y., Negishi, N., Ogata, A., 2015. A multi disciplinary approach to
847 understand the interactions of non-thermal plasma and catalyst: A review. Catal. Today
848 256, 13–22. https://doi.org/10.1016/j.cattod.2015.04.009.
849 Lee, B., Park, S., Lee, S., Kang, M., Choung, S., 2004. Decomposition of benzene by using a
850 discharge plasma – photo-catalyst hybrid system 95, 769–776.
851 https://doi.org/10.1016/j.cattod.2004.06.069.
852 Li, D., Yakushiji, D., Kanazawa, S., Ohkubo, T., Nomoto, Y., 2002. Decomposition of toluene
853 by streamer corona discharge with catalyst 55, 311–319.
854 Li, D., Yakushiji, D., Kanazawa, S., Ohkubo, T., Nomoto, Y., 2001. Decomposition of Toluene
855 by Using a Streamer Discharge Reactor Combined with Catalysts 00, 1077–1081.
856 Li, Y., Guan, D., Tao, S., Wang, X., He, K., 2018. A review of air pollution impact on
857 subjective well-being : Survey versus visual psychophysics. J. Clean. Prod. 184, 959–
858 968. https://doi.org/10.1016/j.jclepro.2018.02.296.
859 Liang, W., Li, Jian, Li, Jing-xin, Zhu, T., Jin, Y., 2010. Formaldehyde removal from gas
860 streams by means of NaNO 2 dielectric barrier discharge plasma 175, 1090–1095.
861 https://doi.org/10.1016/j.jhazmat.2009.10.034.
862 Lin, Y., Hsueh, H., Chang, C., Chu, H., 2016. The visible light-driven photodegradation of
863 dimethyl sulfide on S-doped TiO 2 : characterization , kinetics , and. """Applied Catal. B,
864 Environ. https://doi.org/10.1016/j.apcatb.2016.06.024.
865 Linga, J.K.E., Manoj, R.P., Reddy, K., 2014. Catalytic non-thermal plasma reactor for the
866 abatement of low concentrations of benzene 311–318. https://doi.org/10.1007/s13762-
867 013-0218-z.
868 Liu, H., Yu, X., Yang, H., 2014. The integrated photocatalytic removal of SO 2 and NO using
869 Cu doped titanium dioxide supported by multi-walled carbon nanotubes. Chem. Eng. J.
870 243, 465–472. https://doi.org/10.1016/j.cej.2014.01.020.
871 Lu, S., Chen, L., Huang, Q., Yang, L., Du, C., Li, X., Yan, J., 2014. Chemosphere
872 Decomposition of ammonia and hydrogen sulfide in simulated sludge drying waste gas
873 by a novel non-thermal plasma. Chemosphere 117, 781–785.

https://doi.org/10.1016/j.chemosphere.2014.10.036.
Ma, J., He, H., Liu, F., 2015. Environmental Effect of Fe on the photocatalytic removal of NO x over visible light responsive Fe / TiO 2 catalysts. """Applied Catal. B, Environ. 179, 21–28. https://doi.org/10.1016/j.apcatb.2015.05.003.
Magureanu, M., Bogdan, N., Hu, J., Richards, R., Florea, M., Parvulescu, M., 2007. Plasma-assisted catalysis total oxidation of trichloroethylene over gold nano-particles embedded in SBA-15 catalysts. Catal. B envirenmental 76, 275–281. https://doi.org/10.1016/j.apcatb.2007.05.030.
Martin, L., Ognier, S., Gasthauer, E., Cavadias, S., Dresvin, S., Amouroux, J., 2008. Destruction of Highly Diluted Volatile Organic Components (VOCs) in Air by Dielectric Barrier Discharge and Mineral Bed Adsorption 576–582.
Maxime, G., Amine, A.A., 2014. Removal of gas-phase ammonia and hydrogen sulfide using photocatalysis , non-thermal plasma , and combined plasma and photocatalysis at pilot scale 13127–13137. https://doi.org/10.1007/s11356-014-3244-6.
Mei, D., Zhu, X., Wu, C., Ashford, B., Williams, P.T., Tu, X., 2016. Plasma-photocatalytic conversion of CO 2 at low temperatures : Understanding the synergistic effect of plasma-catalysis.
Mizuno, A., 2007. Industrial applications of atmospheric non-thermal plasma in environmental remediation. Plasma Phys. Control. Fusion 49, A1–A15. https://doi.org/10.1088/0741-3335/49/5A/S01.
Monteiro, R.A.R., Miranda, S.M., Rodrigues-silva, C., Faria, J.L., Silva, A.M.T., Boaventura, R.A.R., Vilar, V.J.P., 2015. Gas phase oxidation of n-decane and PCE by photocatalysis using an annular photoreactor packed with a monolithic catalytic bed coated with P25 and PC500. Appl. Catal. B Environ. 165, 306–315.
Murali, A., Sarswat, P.K., Sohn, H.Y., 2019. Enhanced photocatalytic activity and photocurrent properties of plasma-synthesized indium-doped zinc oxide nanopowder. Mater. Today Chem. 11, 60–68. https://doi.org/10.1016/j.mtchem.2018.10.007.
Murcia, J.J., Hidalgo, M.C., Vaiano, V., Sannino, D., Ciambelli, P., 2013. Cyclohexane photocatalytic oxidation on Pt/TiO2 catalysts. Catal. Today. https://doi.org/10.1016/j.cattod.2012.11.018.
Maciuca, A., Batiot-Dupeyrat, C., Tatibouët ,J.M., 2012. Synergetic effect by coupling photocatalysis with plasma for low VOCs concentration removal from air. Appl. Catal. B Environ. 432-438.
Mikhail N.Lyulyukin ,Alexey S.Besov, Alexander V.Vorontsov. 2016. Acetone and ethanol vapor oxidation via negative atmospheric corona discharge over titania-based catalysts. Applied Catalysis B: Environmental, 18-27https://doi.org/10.1016/j.apcatb.2015.10.025.
Neyts, E.C., 2016. Plasma-Surface Interactions in Plasma Catalysis. Plasma Chem. Plasma

Process. 36, 185–212. https://doi.org/10.1007/s11090-015-9662-5

Nan Jiang, Ke-Feng Shang, Na Lu, Hu Li, Jie Li, and Yan Wu High-Efficiency , 2016.Removal of NOx From Flue Gas by Multitooth Wheel-Cylinder Corona Discharge Plasma Facilitated Selective Catalytic Reduction Process, IEEE Transactions on Plasma Science 2738- 2744

https://doi.org/ 10.1109/TPS.2016.2609140

Nguyen Dinh M.T., Giraudon J.M., Vandenbroucke A.M., Morent R., De Geyter N., Lamonier J.F., « Post plasma-catalysis for total oxidation of trichloroethylene over Ce-Mn based oxides synthesized by a modified Bredox-precipitation route ». Applied Catalysis B: Environmental (2015) 65-72

Ondarts, M., Hajji, W., Outin, J., Bejat, T., Gonze, E., 2016. Non-Thermal Plasma for indoor air treatment: Toluene degradation in a corona discharge at ppbv levels. Chem. Eng. Res. Des. https://doi.org/10.1016/j.cherd.2016.12.015

Palau, J., Assadi, A.A., Penya-roja, J., Bouzaza, A., Wolbert, D., Martínez-Soria, V., 2015. Isovaleraldehyde degradation using UV photocatalytic and dielectric barrier discharge reactors, and their combinations.

Pham Huu T., Sivachandiran L., Da Costa P., Khacef A., « Methane, Propene and Toluene Oxidation by Plasma-Pd/c-Al2O3 Hybrid Reactor: Investigation of a Synergetic Effect ». Top. Catal. (2017) 326-332

Pham, T., Lee, B., 2015. Novel adsorption and photocatalytic oxidation for removal of gaseous toluene by V-doped TiO 2 / PU under visible light. J. Hazard. Mater. 300, 493–503. https://doi.org/10.1016/j.jhazmat.2015.07.048

Pham Huu T., Gil S., Costa P.D., Giroir-Fendler A., Khacef A., « Plasma-catalytic hybrid reactor: Application to methane removal ». Catalysis Today (2015) 86-92

Portela, R., Rasmussen, S.B., Arconada, N., Castro, Y., Coronado, J.M., 2010. Photocatalytic-based strategies for H2S elimination. Catal. TodayToday. https://doi.org/10.1016/j.cattod.2010.03.056

Portela, R., Sánchez, B., Coronado, J.M., 2007. Photocatalytic Oxidation of H2S on TiO2 and TiO2 -ZrO2 Thin Films 10, 375–380.

Ramaraju, B., Subrahmanyam, C., 2014. Catalytic non-thermal plasma reactor for stripping the VOCs from air 37–41. https://doi.org/10.1080/15685543.2014.927716

Ray, D., Subrahmanyam, C., 2016. CO 2 decomposition in a packed DBD plasma reactor : in fl uence of packing materials †. RSC Adv. 6, 39492–39499. https://doi.org/10.1039/C5RA27085E

Rousseau, A., Guaitella, O., Gatilova, L., Paris, O. De, Thevenet, F., 2005. Photocatalyst activation in a pulsed low pressure discharge. https://doi.org/10.1063/1.2136415

947 Sun, K., YanSongbFalinHeaMingyangJingaJingchunTangcRutaoLiua2021. A review of
948 human and animals exposure to polycyclic aromatic hydrocarbons: Health risk and
949 adverse effects, photo-induced toxicity and regulating effect of microplastics, Science of
950 The Total Environment, 773, 145403. https://doi.org/10.1016/j.scitotenv.2021.145403

951 Sano, T., Negishi, N., Sakai, E., Matsuzawa, S., 2006. Contributions of photocatalytic /
952 catalytic activities of TiO 2 and Al 2 O 3 in non-thermal plasma on oxidation of
953 acetaldehyde and CO 245, 235–241. https://doi.org/10.1016/j.molcata.2005.10.002
954
955 Sultana,S, Vandenbrouckea, A.M., Morab, M., Jiménez-Sanchidriánb, C., Romero-
956 Salguerob,Leysa, F.J.C, Geytera, N.De, Morenta, R. 2019. Post plasma-catalysis for
957 trichloroethylene decomposition over CeO2 catalyst: Synergistic effect and stability test
958 Applied Catalysis B: Environmental 49-59 https://doi.org/10.1016/j.apcatb.2019.03.077.
959
960 Sivachandiran L., Thevenet F., Gravejat P., Rousseau A., « Isopropanol saturated TiO2
961 surface regeneration by non-thermal plasma: influence of air relative humidity ». Chem.
962 Eng. J. (2013) 17-26
963 Saoud W., Kane A, Le Cann P., Gerard A., Lamaa L., Peruchon L., Brochier C., Bouzaza A.,
964 Wolbert D., Assadi A. A., 2021, Innovative photocatalytic reactor for the degradation of
965 VOCs and microorganism under simulated indoor air conditions: Cu-Ag/TiO2-based
966 optical fibers at a pilot scale, Chemical Engineering Journal, 411, 128622,
967 https://doi.org/10.1016/j.cej.2021.128622.
968 Saoud, W.A., Assadi, A.A., Guiza, M., Bouzaza, A., Aboussaoud, W., Ouederni, A., Soutrel,
969 I., Saoud, W.A., Assadi, A.A., Guiza, M., Bouzaza, A., Aboussaoud, W., 2017. Study of
970 synergetic effect , catalytic poisoning and regeneration using dielectric barrier discharge
971 and photocatalysis in a continuous reactor : Abatement of pollutants in air mixture
972 system To cite this version : HAL Id : hal-01542763.
973 Saoud, W.A., Assadi, A.A., Guiza, M., Bouzaza, A., Aboussaoud, W., Ouederni, A., Wolbert,
974 D., Rtimi, S., Saoud, W.A., Assadi, A.A., Guiza, M., Bouzaza, A., Aboussaoud, W.,
975 2018. Abatement of ammonia and butyraldehyde under non-thermal plasma and
976 photocatalysis Oxidation processes for the removal of mixture pollutants at pilot scale
977 To cite this version : HAL Id : hal-01774403. Chem. Eng. J.

https://doi.org/10.1016/j.cej.2018.03.068

Saoud, W.A., Assadi, A.A., Guiza, M., Loganathan, S., Bouzaza, A., Aboussaoud, W., Ouederni, A., Rtimi, S., Wolbert, D., 2019. Synergism between non-thermal plasma and photocatalysis Implicationsin the post discharge of ozone at a pilot scale in a catalytic fixed-bed reactor. """Applied Catal. B, Environ. 227–235. https://doi.org/10.1016/j.apcatb.2018.09.029

Saoud, W.A., Assadi, A.A., Kane, A., Jung, A., Cann, P. Le, Bazantay, F., Bouzaza, A., Wolbert, D., 2020. Integrated process for the removal of indoor VOCs from food industry manufacturing Elimination of Butane-2,3-dione and Heptan-2-one by cold plasma-photocatalysis combination. Photochem. Photobiol. A Chem. 386,112071.

Schiavon, M., Torretta, V., Casazza, A., Ragazzi, M., 2017. Non-thermal Plasma as an Innovative Option for the Abatement of Volatile Organic Compounds : a Review. https://doi.org/10.1007/s11270-017-3574-3

Schmidt, M., Jo, I., 2015. Non-thermal plasma based decomposition of volatile organic compounds in industrial exhaust gases 3745–3754. https://doi.org/10.1007/s13762-015-0814-1

Subrahmanyam, C., 2009. Catalytic non-thermal plasma reactor for total oxidation of volatile organic compounds 48, 1062–1068.

Subrahmanyam, C., Magureanu, M., Laub, D., Renken, A., 2007. Nonthermal Plasma Abatement of Trichloroethylene Enhanced by Photocatalysis 4315–4318.

Subrahmanyam, C., Renken, A., Kiwi-minsker, L., 2010. Catalytic non-thermal plasma reactor for abatement of toluene. Chem. Eng. J. 160, 677–682. https://doi.org/10.1016/j.cej.2010.04.011

Sun, R., Ã, Z.X., Chao, F., Zhang, W., Zhang, H., Yang, D., 2007. Decomposition of low-concentration gas-phase toluene using plasma-driven photo-catalyst reactor 41, 6853–6859. https://doi.org/10.1016/j.atmosenv.2007.04.041

Szatmáry, L., Subrt, J., Kalousek, V., 2014. Low-temperature deposition of anatase on nanofiber materials for photocatalytic NO x removal 230, 74–78.

Shi Y., Shao Z., Shou T., Tian R., Jiang J., He Y., 2016. Abatement of Gaseous Xylene Using Double Dielectric Barrier Discharge Plasma with In Situ UV Light: Operating Parameters and Byproduct Analysis ». Plasma Chem Plasma Process 1501-1515.

Shirjana Saud, Duc Ba Nguyen, Seung-Geon Kim, Ho Won Lee, Seong Bong Kim and Young Sun Mok, 2020. Improvement of Ethylene Removal Performance by Adsorption/Oxidation in a Pin-Type Corona Discharge Coupled with Pd/ZSM-5 Catalyst, Catalysts, 10, 133 https://doi:10.3390/catal10010133.

Taranto, J., Frochot, D., Pichat, P., 2007. Combining Cold Plasma and TiO 2 Photocatalysis To Purify Gaseous Effluents : A Preliminary Study Using Methanol-Contaminated Air 7611–7614.

Thevenet, F., Guaitella, O., Puzenat, E., Guillard, C., Rousseau, A., 2008. Environmental Influence of water vapour on plasma / photocatalytic oxidation efficiency of acetylene. Catal. B. https://doi.org/10.1016/j.apcatb.2008.06.029.

Thevenet, F., Guaitella, O., Puzenat, E., Herrmann, J., 2007. Oxidation of acetylene by photocatalysis coupled with dielectric barrier discharge 122, 186–194. https://doi.org/10.1016/j.cattod.2007.01.057.

Thevenet, F., Guillard, C., Rousseau, A., 2014. Acetylene photocatalytic oxidation using continuous flow reactor : Gas phase and adsorbed phase investigation , assessment of the photo-catalyst deactivation. Chem. Eng. J. 244, 50–58. https://doi.org/10.1016/j.cej.2014.01.038.

Trinh, Q.H., Mok, Y.S., 2015. Non-Thermal Plasma Combined with Cordierite-Supported Mn and Fe Based Catalysts for the Decomposition of Diethylether 800–814. https://doi.org/10.3390/catal5020800.

Vandenbroucke, A.M., Dinh, M.T.N., Nuns, N., Giraudon, J., Geyter, N. De, Leys, C., Lamonier, J., Morent, R., 2016. Combination of non-thermal plasma and Pd / LaMnO 3 for dilute trichloroethylene abatement. Chem. Eng. J. 283, 668–675. https://doi.org/10.1016/j.cej.2015.07.089.

Visscher, A. De, Dewulf, J., Durme, J. Van, Leys, C., Morent, R., Langenhove, Van, H., 2008. Non-thermal plasma destruction of allyl alcohol in waste gas: kinetics and

1035 modelling. Plasma Sources Sci. Technol. 17, 015004–015015.
1036 https://doi.org/10.1088/0963-0252/17/1/015004.
1037 Wan, Y., Fan, X., Zhu, T., 2011. Removal of low-concentration formaldehyde in air by DC
1038 corona discharge plasma. Chem. Eng. J. 171, 314–319.
1039 https://doi.org/10.1016/j.cej.2011.04.011
1040 Wang, P., Chen, J., 2009. Numerical modelling of ozone production in a wire – cylinder
1041 corona discharge and comparison with a wire – plate corona discharge 035202.
1042 https://doi.org/10.1088/0022-3727/42/3/035202.
1043 Xie, H., Liu, B., Zhao, X., 2015. Facile process to greatly improve the photocatalytic activity
1044 of the TiO 2 thin film on window glass for the photodegradation of acetone and benzene.
1045 Chem. Eng. J. https://doi.org/10.1016/j.cej.2015.09.049.
1046 Xu, X., Wu, J., Xu, W., He, M., Fu, M., Chen, L., 2016. High-efficiency non-thermal plasma-
1047 catalysis of cobalt incorporated mesoporous MCM-41 for toluene removal. Catal. Today.
1048 https://doi.org/10.1016/j.cattod.2016.03.036.
1049 Ye, G.Y., Tian, D.C.K., 2006. Humidity Effect on Toluene Decomposition in a Wire-plate
1050 Dielectric Barrier Discharge Reactor 237–249. https://doi.org/10.1007/s11090-006-
1051 9008-4.

1052 Zhang, Z., 2018. Emission and health risk assessment of volatile organic compounds in
1053 various processes of a petroleum refinery in the Pearl River Delta, China, Environmental
1054 Pollution 238, 452-461. https://doi.org/10.1016/j.envpol.2018.03.054.

1055 Zadi, T., Assadi, A.A., Nasrallah, N., Bouallouche, R., Tri, P.N., Bouzaza, A., Azizi, M.M.,
1056 Maachi, R., Wolbert, D., 2018. Treatment of hospital indoor air by a hybrid system of
1057 combined plasma with photocatalysis: Case of trichloromethane. Chem. Eng. J. 349,
1058 276–286. https://doi.org/10.1016/j.cej.2018.05.073.
1059 Zadi, T., Azizi, M., Nasrallah, N., Bouzaza, A., Maachi, R., 2020. Indoor air treatment of
1060 refrigerated food chambers with synergetic association between cold plasma and
1061 photocatalysis : Process performance and photocatalytic poisoning To cite this version :

1062 HAL Id : hal-02386052.
1063 Zhu, T., Li, J., Jin, Y.Q., 2009. Gaseous phase benzene decomposition by non-thermal
1064 plasma coupled with nano titania catalyst 6, 141–148.
1065 Zhuang, H., Gu, Q., Long, J., Lin, Huan, Lin, Huaxiang, Xuxu Wang, 2014. Visible light-
1066 driven decomposition of gaseous benzene on robust Sn2+-doped anatase TiO2
1067 nanoparticles. RSC Adv. https://doi.org/10.1039/x0xx00000x.
1068 Zhu, X., Gao, X., Qin, R., Zeng, Y., Qu, R., Zheng, C., 2015a .Plasma-catalytic removal of
1069 formaldehyde over CuCe catalysts in a dielectric barrier discharge reactor. Applied
1070 Catalysis B: Environmental 293-300.

From Initial Idea...

Tubular Reactor

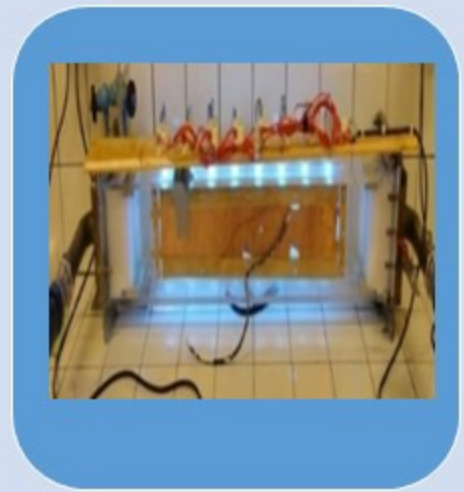

Planar Reactor

Photocatalysis+Plasma